Pitfalls in reservoir monitoring with CSEM

K. Strack [1], S. Davydycheva[1,] A.Y. Paembonan[2]

[1] KMS Technologies – Houston, Texas
[2]Engineering Geophysics, Sumatera Institute of Technology, Indonesia
email: Kurt@kmstechnologies.com

ABSTRACT

Electromagnetic (EM) method, especially Controlled Source Electromagnetic (CSEM) are a unique way of observing fluid movement at depth from the surface. The depth range of interest for hydrocarbon and geothermal applications is from about 500m to 5-7 km. For hydrocarbon reservoirs monitoring we focus to improve the recovery factors and understand fluid movement resulting in lower carbon footprint per produced barrel of oil. For geothermal applications, we can observe magma movements as aid for volcano eruption prediction or monitor producing geothermal field to improve production efficiency and to observe (in correlation with microseismic) reservoir damage and potential induced seismicity.

To see percentage level variations, more detailed attention is required at all data handling stages. During acquisition, more effort is required to obtain long term stable transmitter and receiver sites including not only daily monitoring of contact resistance but also controlling them during the acquisition process to better than 1% variations. Because of the large dynamic range of the signal, a highly accurate reference level with active adjustment before the transmitted signal is necessary. While processing the data, a feedback loop between filter selection and noise suppression in the reservoir signal band allows you to optimize the filter and to reduce their effect on the anomaly itself. For a sedimentary environment, anisotropy is the biggest cause for error and misinterpretation. It is derived before the survey from existing logs using end members derived from the resistivity log based on the interaction of the layers on reservoir scale.

Another serious issue is the image focus. In principle, we assume the information comes from underneath the receiver but for different measurements it comes from various volume between transmitter and receiver. As with focusing of laterologs, we use a focusing method either by differential measurements or additional borehole receivers.

We are using real field measurements as example for potential misinterpretation to illustrate the severance of these issues.

INTRODUCTION

Advanced EM survey can identify the formation's petrophysical properties from electrical parameters related to the behavior of fluid movement. For geothermal/hydrocarbon applications it gives even higher value during the production than the exploration stage.

CSEM is important for hydrocarbon and geothermal reservoirs monitoring to improve recovery factors and to observe fluid movement induced reservoir changes. It can be compared to monitoring magma movements and aid for volcano eruption prediction. This requires stable equipment (transmitter and receiver) and even higher accuracy of processing to increase signal-to-noise ratio by applying the filter the data pre-stack and post-stack as well as stacking (Paembonan et al., 2017).

In reservoir monitoring, electrical property changes appear at the reservoir fluid boundaries. The larger the contrast, the larger is the electromagnetic (EM) response. Thus, EM methods provide unique opportunities to track fluid movements and flow. They are important parameters in reservoir management, especially for high value targets such as unconventional (shale) reservoirs or steam/water/CO_2 flood EOR. Thus, the EM data and interpretation could yield considerably more value than traditional seismic interpretation alone. At the same time, technology has progressed such that it is now routine recording virtually an unlimited number of channels at lower cost (than in the past) and interpreting data in 3D.

Surface-to-surface Controlled Source EM (CSEM) applications using a grounded electric dipole in time-domain (Strack, 1992; 2004, 2014; Strack & Aziz, 2013) are more promising for land applications than frequency domain CSEM (Johansen et al., 2005; Constable, 2010), since it is advantageous to record once the transmitter is off, after the airwave has passed (Kumar & Hoversten, 2012).

Reservoir monitoring is a time-lapse exercise with measurements that link downhole and surface-to-surface data enable critical calibration and increasing sensitivity to fluid variations in the reservoir. The wealth of EM information tied to 3D surface and borehole seismic data also permits to extrapolate fluid movements and seal integrity away from a given well bore (Passalacqua et al. 2016). To date, EM applications for reservoir monitoring are in an early stage of development. Presently, only limited monitoring applications have been reported (Hoversten et al. 2015, Tietze et al. 2014; 2015; Thiel, 2016).

Over the past 10 years we have be developing an array system concept that includes the combination of surface and borehole measurements (Strack, 2004). When realizing that the existing geophysical system did not meet our requirements, we developed an integrated borehole, marine and land concept with the survey layout shown in Figure 1. On the right of the figure is the typical 3D layout where data is acquired in 16/25 station bins with only one complete set of magnetic fields. In the center is the rough terrain layout where a complete station is carried in (or by helicopter/drone). On the left of the figure are sparser spaced 2D lines with all components at each site. From borehole measurements and the recent 3D induction logging tools, it became apparent that borehole resistivity logs in anisotropic formations (most basins) are underestimating hydrocarbon reserves by more than 25% (Yu et al., 2001; Barber et al., 2004). Figure 2 shows two log examples with the one from Yu et al. (2001) on the left and from Barber et al. (2004) on the right. Shown are the resistivity logs (obtained after first inverting the raw data) with the supporting logs and subsequent shaly sand analysis. In both case the increased reserved that were estimated from the 3-component induction log was more than 40%, more than from the normal induction log that only measures horizontal resistivity and it is dominated by shales. This means that if we ignore the vertical resistivity we make and error in oil reserved by more than 40%. We experienced similar effects for marine controlled source electromagnetics when ignoring transverse-isotropic anisotropy (Thomsen et al., 2007). This results in the requirement of measuring full tensor resistivities in the borehole and on the surface.

As novel contribution, we derived a methodology and additional measurements where the information content can be focused below the receivers using either Focused Source EM (FSEM) (Davydycheva & Rykhlinski, 2009; 2011) or vertical electric field measurements. This will overcome the issue with not knowing the image point where the information comes from that we measure at the receiver site.

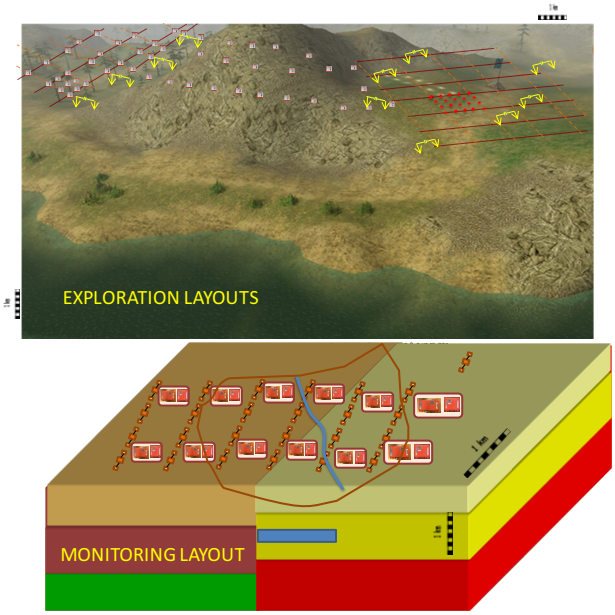

Figure 1: Field layout for carrying out CSEM land surveys (top) and monitoring measurements (bottom).

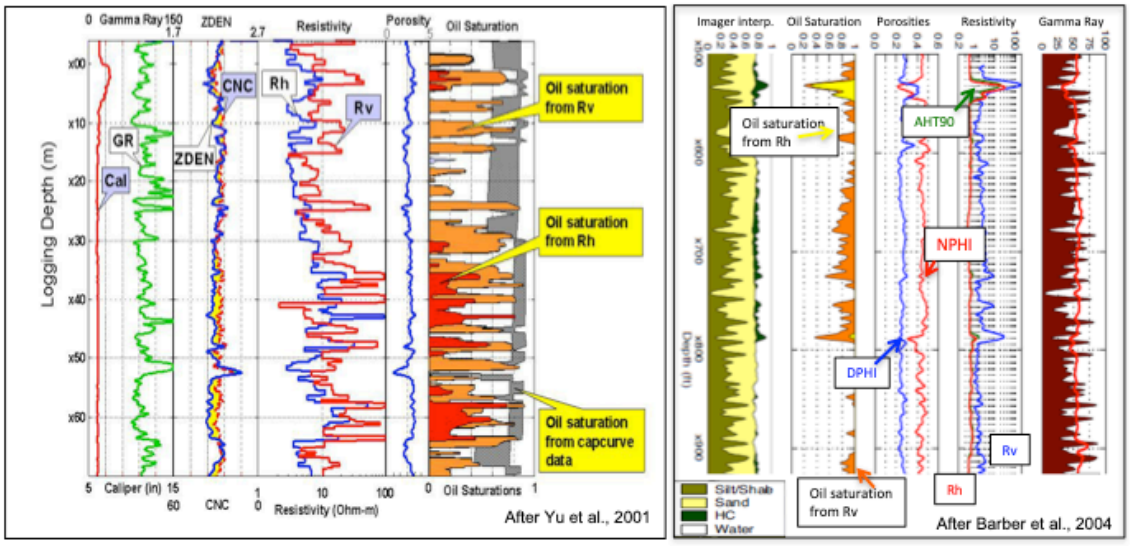

Figure 2: Two examples of interpreted 3D induction logs using 3-component transmitter and receivers. In both cases the improved oil saturation is shown in the orange shaded track.

ACQUSITION ISSUES

From the acquisition side, for reservoir monitoring, the main issue is source stability, high power and accurate synchronization between transmitter and receiver. Since we use a grounded dipole the latter also depends on the inductance and resistance of the source. When addressing this correctly in the hardware, we experienced that – with active current control – this can be kept at below 0.5% source repeatability over long periods of time.

The processing steps including pre-stacking, stacking, and post-staking, were done because most of the time, the electromagnetic noise is much bigger than the signals, so that the recorded time series must be processed before interpretation. This processing includes certain steps:

1. Filtering each time series separately to reduce the periodic cultural noise, mostly from power lines,
2. Stacking all-time series selectively to reduce aperiodic noise,
3. Smoothing the stacked data using recursive average filter, while the DC level is corrected.
4. Normalizing both the electric and the magnetic fields by the transmitter and receiver dipole moments, or converted to the apparent resistivities for further inversion.

Similar workflows can be found in Strack et al. (1989), Strack (1992) and Hoerdt et al. (2000). Figure 3 shows a workflow summary for the data used herein (Paembonan et al., 2017). In addition, a feedback-loop between filter selection and time window was introduced to keep all filtering effects outside the reservoir window.

As mentioned above, extreme care must be taken in building a very stable transmitter electrode plant and controlling the current to an accuracy better than 0.5%. There are two sets of synchronization used for the data. One is the GPS time stamp with the data which is the same everywhere. The other is the current switching where the waveform is generated by the transmitter controller. While it is obvious that they must be accounted for, it is NOT obvious that they vary based on transmitter inductance and the delay between the GPS pulse and source timing waveform because the signal response depends on the actual current switching. Time synchronization of the transmitter and receiver data generally means that the data from these two devices (the receiver and the transmitter) have the same start time, the higher this error, the higher the inaccuracy in subsurface response as shown in Figure 4. The transmitter signal in blue comes before the receiver signal, both have different delays due to different recording sensors. The total uncertainty in start can translate to almost a factor of 10 in voltage variation be selecting an onset time 83 msec different. The unusual high value shows that we need to monitor this difference a select a consistent time. The shift depends also – to a lesser degree – on the inductance of the dipole which for 1 km dipoles is in the order of 10 mH. We observed chances with quality of the transmitter.

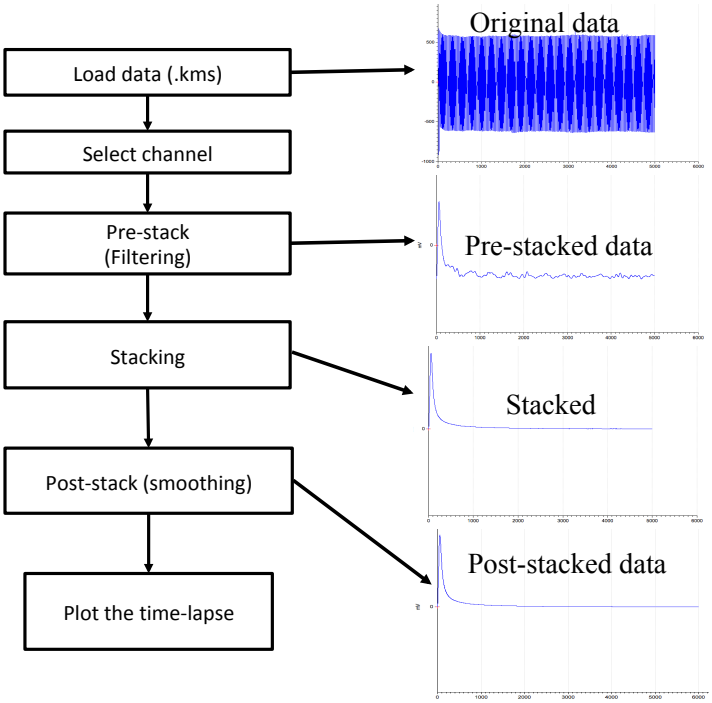

Figure 3: Workflow example for the monitoring data in the example.

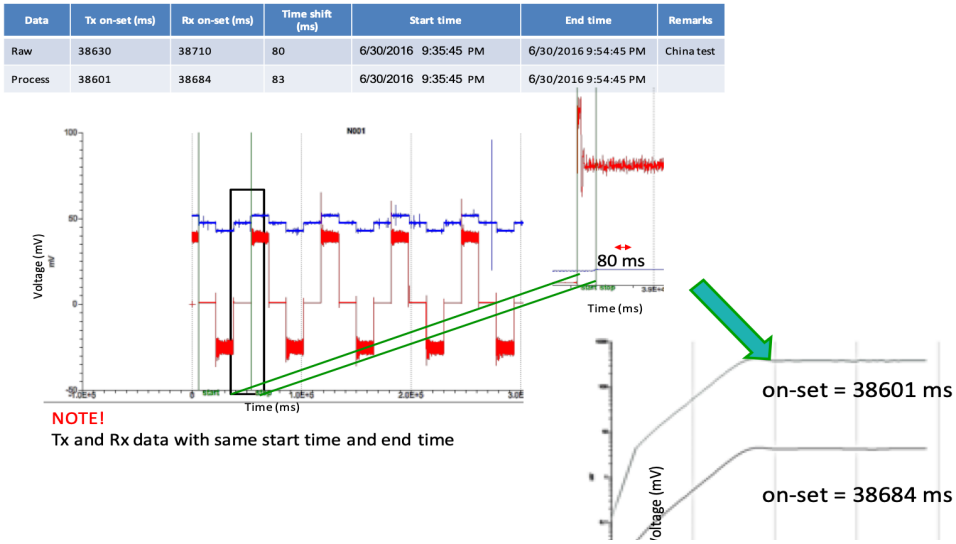

Figure 4: An example of time alignment effect due to uncertainty current switching for transmitter (red) and receiver data (blue).

Another big error stems from the inherent inaccuracy of image focus related to the receiver location. In borehole logging this is handle by focusing the injected current to a narrow bed (c.f. focused logs). We apply these principles described by Davydycheva & Rykhlinski (2009; 2011) which are equivalent to log focusing where we take the different measurements of two transmitters. Instead of using many sources we can also use multiple receivers by applying the principle-of-reciprocity. Figure 53 shows sensitivity plots for time

and frequency domain on the left and on the right for focused source EM (also for time and frequency). The FSEM on the right shows that by build the differences between receivers we get the vertical current from below.

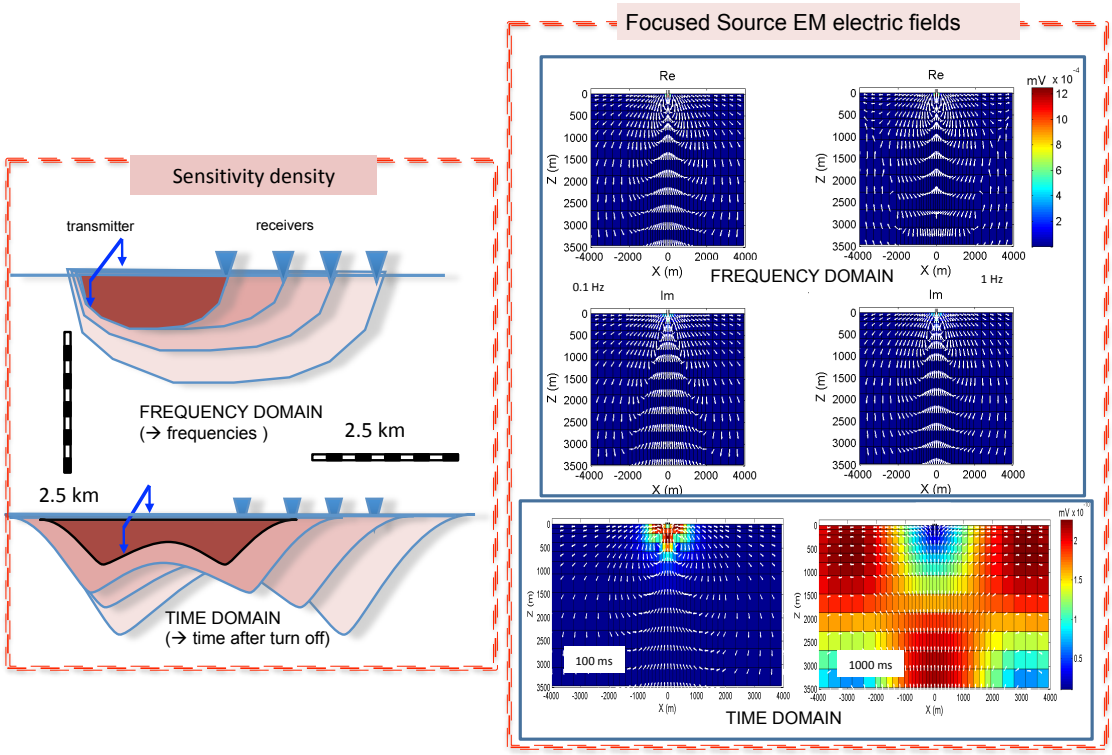

Figure 5: Two dimensional sensitivity plots for time and frequency domainmeasurements from a grounded dipole (left). On the right are the differential current flows for equivalent frequency or time windows shown.

The electric fields on the right of the figure shown indicate current flow showing pre-dominantly vertical flow below the receivers resulting from differential FSEM measurements. This means that the measurements are sensitive directly below the receiver site compared to spread out volume on the left side of the figure for normal CSEM setups.

RESERVOIR MONITORING

We applied a 195-channel system shown in Figure 6 (top) with a 100 KVA transmitter (bottom) to EOR reservoir monitoring. Like geothermal applications the target was conductive due to water injection. A sample data set is shown in Figure 7 with the electric field at surface followed by the vertical magnetic field and the 3-component seismic data.

The time-lapse processing was applied. The result is displayed in percentage differences from different days of measurements with the purpose of obtaining the resistivity changes representing reservoir water flooding. When calculating relative differences, we ensured that filter effects stay outside of the reservoir time window. Hence, the time-lapse results are expected to displayed in percentage variation in Figure 8. There were several receiver sites (not shown), only one directly above the water injection and one at the end of the receiver line are shown. Directly above the water flood we can see up to 30%-time lapse variation but 400 m away at the surface the time lapse response disappears in the noise. The observed anomaly at the center is about 30% and when it disappears in the noise about 2%. The response from the 3D model are one order of magnitude smaller. We modeled casing effects and transmitter current channels but could explain this. One way to explain it is by channeling of the electromagnetic current into the water flood itself causing focusing below the receiver.

Thus, we consider in the next section an example on image focusing.

Figure 6 The electromagnetic acquisition system for monitoring example showing transmitter and the 195 channel receivers.

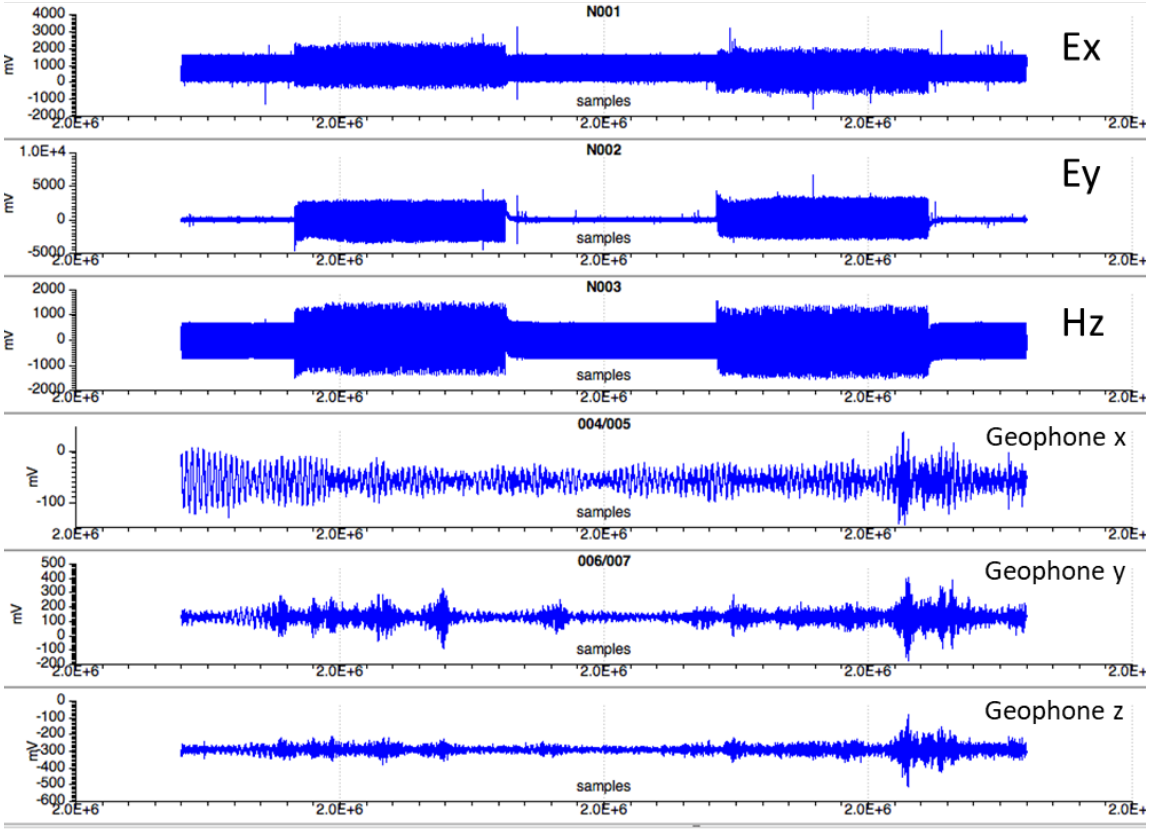

Figure 7: Raw data example of EM reservoir monitoring showing the EM data in the top 3 traces followed by the 3-C seismic data below.

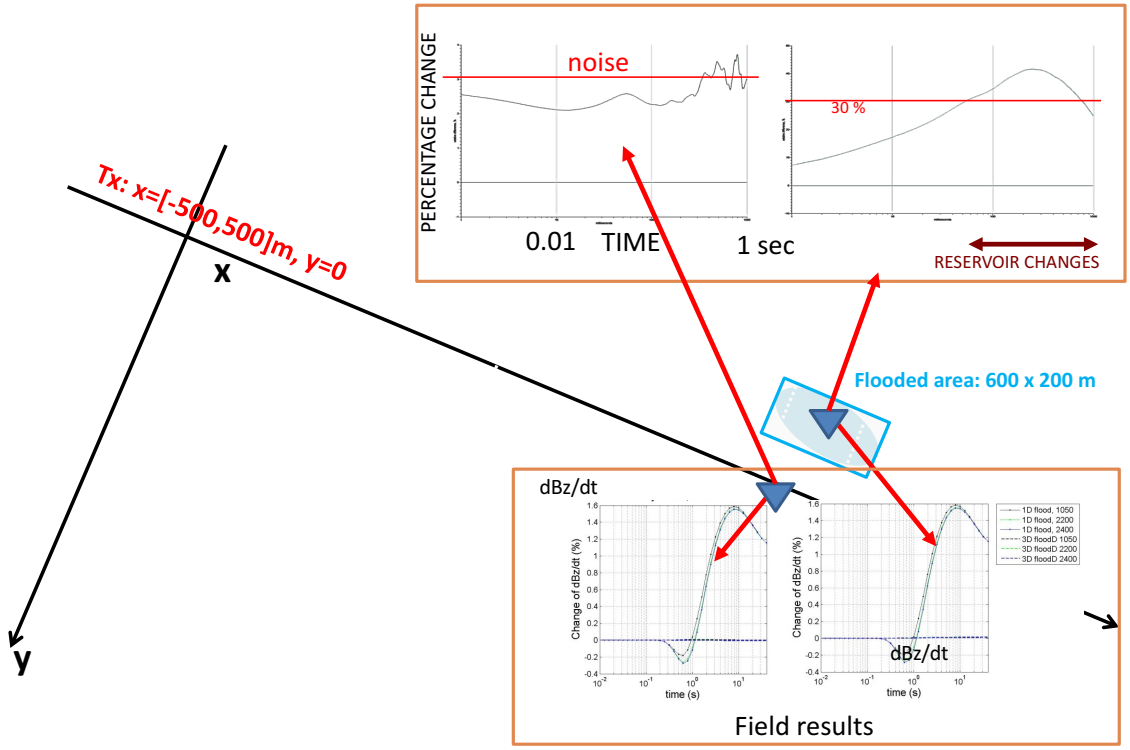

Figure 8: Water-flood monitoring showing the location of the transmitter and receivers and water injection area. At the bottom are the 3D anisotropic models and at the top the field data.

IMAGE FOCUSING USING DATA OVER A SALT DOME

During field tests of the array system, we acquired various data over the Hockley salt dome near Houston, Texas. The location is about 10 km west of Houston near a producing salt mine shown in Figure 9. We used the well-log from a well (Direct Warren) and derive anisotropic resistivity models that were used in all 3D modeling. Apart from various magnetotelluric measurements, we also carried out an FSEM test using a controlled source.

The result from Hockley show that the resistivity contrast between conductive layer and resistive layer can be clearly distinguished from the measurements. The conductive layer in the near surface can be seen in most data set and represents a swampy area. Second layer is defined as the resistive salt layer and underlined by the conductive layer. Meanwhile, the fourth layer show the higher resistivity to the bottom.

Figure 10 shows the result from the CSEM electric fields and the FSEM measurements in comparison with the 3D model responses above the best matching model. The model was obtained via trial and error but we found that it requires the salt overhang. Note that the CSEM measurements on the left match as do the FSEM measurements.

In Figure 11 we show additional Lotem (top) and MT (bottom) inversion for comparison. Both 1D inversions show the salt dome overhang.

SUMMARY

Applying controlled source EM to reservoir monitoring for hydrocarbon/geothermal applications requires accuracy from the instrumentation/measurements beyond what was used before. We need to reconcile surface tensor measurements with borehole measurements to calibrate the data against known reservoir fluid resistivities. By doing so we can see reservoir fluid changes associated with enhanced oil recovery operation. The uncertainty with image focus from CSEM array can be addressed by measuring in a focused

way like what is being done in the logging industry. The shown example is one of the early indications that FSEM works in a 3D geologic environment.

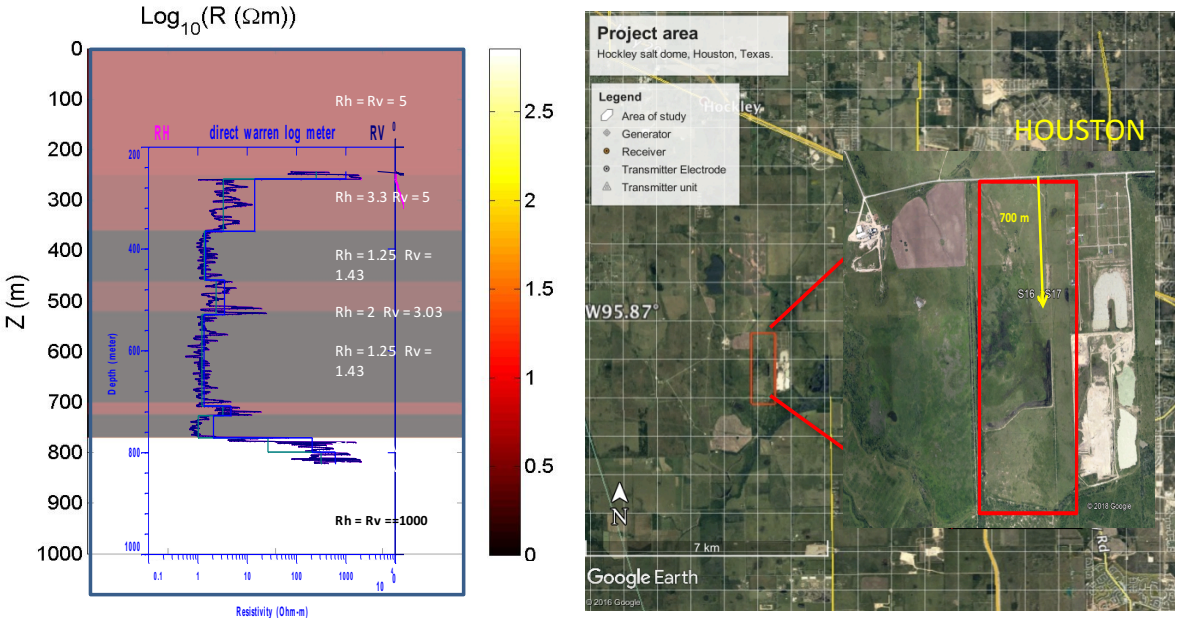

Figure 9: Well log on the left and blocked anisotropic model showing the conductive layer below the salt and the survey location at Hockley salt dome 10 km W of Houston (right). The araows displays theoffset between transmitter and receiver sites.

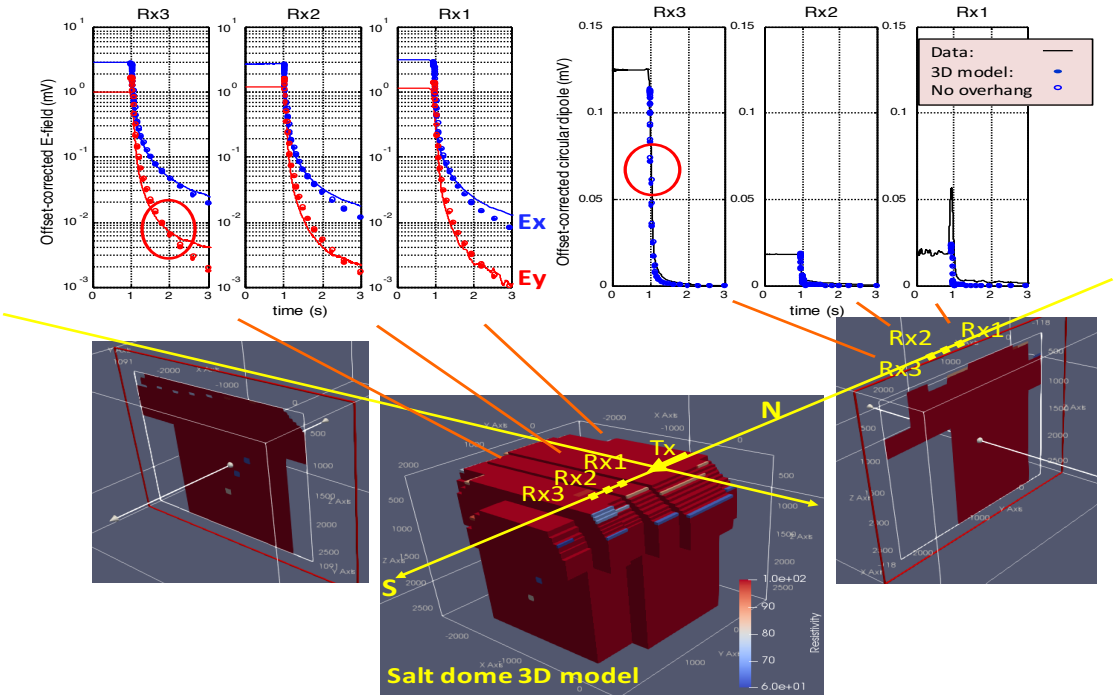

Figure 10: 3D anisotropic model of the Hockley salt dome. The model was obtained through a trial and error process includig geologic constraints.At the top the data (lines) and electrics field model values (dots) are display on the left and on the right the FSEM measurements and model responses. Both shows good agreement.

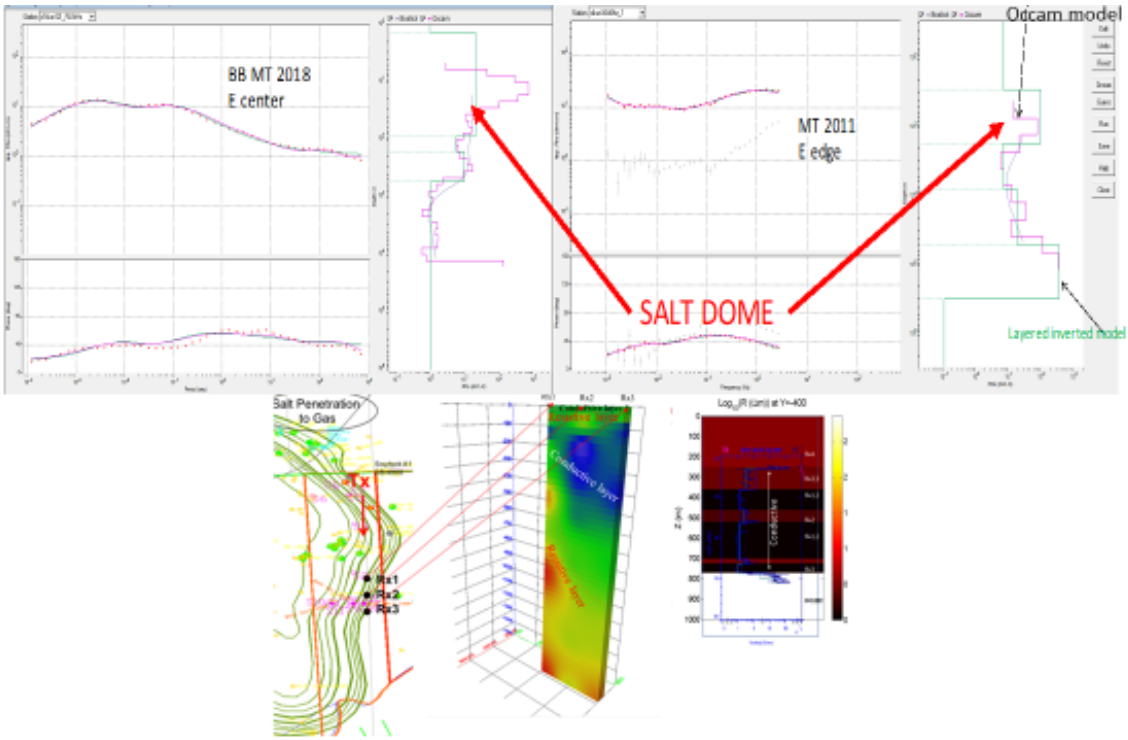

Figure 11 Salt dome interpretation showing the MT inversion resullts (top) and LOTEM inversions (bottom). Both see a resistive salt dome overhang.

REFERENCES

Barber, T.B., Anderson, B., Abubakar, A., Broussard, T., Chen, K-C. , Davydycheva, S., Druskin, V., Habashy, T.M., Homan, D.M., Minerbo, G., Rosthal, R., Schlein, R., & Wang, H., 2004, Determining Formation Resistivity Anisotropy in the Presence of Invasion, Proceedings of SPE Annual Technical Conference, Houston, 26-29 September 2004, Paper 90526.

Constable, S., 2010, Ten years of marine CSEM for hydrocarbon exploration, Geophysics,**75**, A67-A81.

Davydycheva, S. & Rykhlinski, N.I., 2009, Focused Source EM Survey versus time- and frequency-domain CSEM, The Leading Edge, **28**, 944-949.

Davydycheva, S., & Rykhlinski, N.I., 2011, Focused-source electromagnetic survey versus standard CSEM: 3D modeling in complex geometries, *Geophysics,* **76**, F27-F41.

Hördt, A., Andrieux, P., Neubauer, F. M., Rueter, H., & Vozoff, K., 2000, A first attempt at monitoring underground gas storage by means of time-lapse multichannel transient electromagnetics: Geophysical Prospecting, **48**, 489-509.

Hoversten, G.M., Commer, M., Haber, E., & Schwarzbach, C., 2015, Hydro-frac monitoring using ground time-domain electromagnetics, Geophysical Prospecting, **63**, 6, 1508-1526.

Johansen, S.E., Amundsen, H.E.F., Røsten, T., Ellingsrud, S., Eidesmo, T., & Bhuyian, A.H., 2005, Subsurface hydrocarbons detected by electromagnetic sounding: *First Break*, **23**, 31-36.

Kumar, D., & Hovesten, G.M., 2012, Geophysical model response in shale gas, *Geohorizons,***17**, 32-37.

Passalacqua, H., P. Boonyasaknanoon, & K,. Strack, 2016, Integrated Geophysical Reservoir Monitoring for Heavy Oil, Soc. Petr. Eng., SPE-184089-MS.

Paembonan, A.Y., Arjwech, R., Davydycheva, S., & Strack, K. M., A Processing of very noisy LOTEM data from Hockley Salt Dome, Houston, Texas, 2017, 19th EGU General Assembly, Vienna, Austria, 23-28 April, 2017, 6017.

Strack, K.-M., Hanstein, T. H., & Eilenz, H. N., 1989, *LOTEM data processing for areas with high cultural noise levels,* Physics of the Earth and Planetary Interior, **53**, 261-269.

Strack, K. M., 1992, Exploration with deep transient electromagnetics. *Elsevier*, 373 (reprinted 1999).

Strack, K. M., 2004, Combine surface and borehole integrated electromagnetic apparatus to determine reservoir fluid properties, *U. S. Patent 6,739,165*.

Strack, K. M., 2014, Future directionsof Electromagnetic Methods for Hydrocarbon Applications. *Surveys in Geophysics,***35**, 157-177.

Strack, K.M., & Aziz, A.A., 2013, Advances in electromagnetics for reservoir monitoring, *Geohorizons (Special shale issue),* 32-44.

Thiel, S., 2016, Electromagnetic monitoring of hydraulic fracking: relationship to permeability, seismicity and stress, the 23rd Electromagnetic Induction Workshop, Chiang Mai, Thailand, 14-20 August 2016.

Tietze, K., Grayver, A., Streich, R., & Ritter, O. 2014. Recent Developments for Land-based Controlled source EM Surveying, 16 June 2014. *DOI: 10.3997/2214-4609.20140561*.

Tietze, K., Ritter, O., & Veeken, P., 2015, Controlled source electromagnetic monitoring of reservoir oilSaturation using a novel borehole-to-surface configuration, *Geophysical Prospecting,***63**, 1468-1490.

Thomsen, L., Meaux, D., Li, S., Weiss, C. Sharma, A., Allegar, N., & Strack, K., 2007, Novel marine electromagnetics: from deep into shallow water, SEG annual meeting, San Antonio, Recent Advances and Road Ahead session.

Yu, L., Fanini, O. N., Kriegshäuser, B. F., Koelman, J.M.V., & van Popta J. 2001. Enhanced evaluation of low-resistivity reservoirs using new multicomponent induction log data. *Petrophysics*,**42**, 611-623.